Land Use and Land Cover Classification in Google Earth Engine Using Sentinel-2 Based Random Forest: A Case Study of Katsina State, Nigeria

Ismail Dauda Abubakar[1*] and Narayan Vyas[2]

[1, 2]Department of Computer Science and Engineering, Vivekananda Global University, Jaipur, India
[2]Centre of Excellence in Geospatial Technologies for Climate Studies, Vivekananda Global University, Jaipur, India
[1]engrismaildauda@gmail.com
2narayanvyas87@gmail.com

Abstract. Considering the ongoing rapid land transformation across semi-arid sub-Saharan Africa, accurate and up-to-date information on land use and land cover (LULC) is increasingly important for environmental monitoring, agricultural planning, and sustainable land management. No small part of this challenge is captured in Katsina State, northwestern Nigeria, where exacerbating anthropogenic pressures continue to induce significant landscape change but remain largely undocumented in the literature. The study utilized the random forest (RF) machine learning algorithm to map LULC on Katsina State using Sentinel-2 Level-2A surface reflectance imagery collected over the October 2025 late wet-to-dry seasonal transition, processed within the Google Earth Engine (GEE) cloud computing environment. Classification inputs included Sentinel-2 multispectral bands, covering the visible, red-edge, near-infrared, and shortwave-infrared spectral regions. The RF classifier, composed of 100 decision trees, was trained using 80% of the stratified sample points, with the remaining 20% set aside for independent validation. A total of six classes were identified in the LULC data: cropland, vegetation, water, barren, arroyos, and buildup. These led to a confusion matrix-based metric of Overall Accuracy (94.35 %) and standard deviation (0.02851) for classification performance; Vegetation, Cropland, and Water were classified with comparatively higher producer accuracy (100%, 99.36% and 98.45%) while buildup, barren, and arroyos exhibited lower accuracies due to inter-class spectral overlapping under dry season surface conditions. The overall accuracy of 94.35% achieved here is well above that reported for semi-arid LULC classification by single-date images (78-92%), suggesting a better performance of the proposed approach. The results validate that Sentinel-2 imagery and RF classification are a strong and repeatable technique within cloud-based geospatial frameworks, where scalability is limited only by the computing power available in GEE.

Keywords: Land Use and Land Cover (LULC); Random Forest; Sentinel-2; Google Earth Engine (GEE); Remote Sensing Classification; Semi-Arid Environment.

B. Singh et al. (eds.), *Proceedings of the International Conference on Advances in Computing Technology and Artificial Intelligence (COMPUTATIA 2026)*, Atlantis Highlights in Intelligent Systems 18,
https://doi.org/10.2991/978-94-6239-713-2_31

1 Introduction

Remote sensing has been one of the most used tools in monitoring the land surface for more than two decades, and LULC (land use and land cover) classification is a particularly useful application. Especially for the systematic mapping and monitoring of surface features such as water, vegetation, cropland, barren, and arroyos [1]. The Land Use and Land Cover (LULC) information, even though it is more than a map product, is also the foundation of environmental monitoring programs, agronomic policy, sustainable land governance, and resource management decisions at the regional to national level [2]. The study area is situated in the dry-land Sudan Savanna belt of West Africa, a biome that has been gradually but fundamentally modified as a result of population explosion, agricultural encroachment, overgrazing, deforestation, and urbanization [3]. Nevertheless, the region remained under-represented in high-quality LULC studies. Existing studies, however, are limited by time frequency, spatial resolution, or classification methods that do not sufficiently capture the complexity of the area [4], [5].

Machine learning-based remote sensing approaches have proven effective for decision-making for environmental monitoring and land management, as indicated by previous studies [6], [7]. This existing gap is increasingly addressed by utilized Senti-nel-2 dataset, a satellite mission operated by the European Space Agency (ESA) under the Copernicus Programme delivering freely available multispectral imagery at 10 m resolution, which when deployed in tandem with the vast processing capability of cloud-based services such as Google Earth Engine (GEE), allows for LULC mapping at regional scale and reproducibility of methods even in data-limited settings across sub-Saharan Africa [6], [8]. Random forest (RF) has consistent performance for LULC classification in GEE due to its ensemble features, robustness against overfitting, and resistance to spectral noise and band multicollinearity, as demonstrated by these studies [7], [9]. Despite the increasing evidence base, few studies have applied this combined framework to semi-arid landscapes in the northwestern region of Nigeria, where spectral similarity and spatially heterogeneous land-cover classes challenge any classification [10]. This study holistically fills that gap through four objectives: (a) obtaining and preprocessing Sentinel-2 Level-2A of the study area in GEE over an October 2025 late wet-to-dry season window; (b) applying RF-based mapping of six LULC classes including cropland, vegetation, water, barren, arroyos and buildup; (c) assessing classification performance using accuracy assessment methods; and (d) assessing per class performance to identify the source of spectral confusion from potential future improvements across northwestern Nigeria.

2 Study Area and Satellite Data

2.1 Study Area

Katsina state, one of the northwestern states in Nigeria, West Africa was chosen as the study area for this research as shown in Fig. 1. It covers an area of about 24,192

km², is located between latitudes 11°08' to 13°22' North and longitudes 6°52' to 9°02' East, bordered by the Republic of Niger to the north, Kano State to the east, Kaduna State to the south and Zamfara State [11]. Climatologically, the state lies astride the Sudan Savanna ecological area, where a monthly rainfall occurs during a single rainy season between June and September, with an average total of between 500 mm and 900 mm before extended dry harmattan sets in from October to May, which delivers temperatures within the approximate range of 15°C and 45°C [12], [13]. The terrain is mostly flat to gently undulating and crisscrossed by seasonal watercourses, which support both rain-fed farm-cultivations and small-scale irrigation, with agriculture as the economic backbone for more than 70 percent of the population, who grow millet, sorghum, cowpea, groundnut, and cotton [12]. The state provides a suitable area for LULC classification with diverse landscapes, including croplands, woodland savanna, shrublands, grasslands, water, barren, and dispersed buildup settlements [3]. In addition to this natural heterogeneity, intensified anthropogenic pressures such as agricultural dominance, overgrazing, deforestation, and urbanization continuously transform the landscape in the area [14].

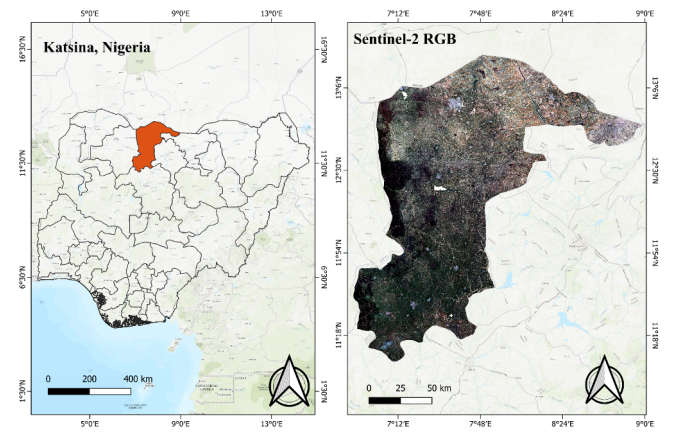

Fig. 1. Administrative Boundary of Katsina State in Nigeria and Its Sentinel-2 Composite Image

2.2 Satellite Data

The main dataset used in this research was Sentinel-2 multispectral imagery obtained from the GEE cloud platform with a coverage filter of less than 10%, acquired from October 1 to October 31, 2025. October was chosen specifically because the late wet-to-dry season transition in Katsina State is a period of vegetative senescence, with harvested fields opened up, and surface water bodies starting to shrink, all factors that

collectively increase spectral differences between land cover types and provide machine learning classifiers with a cleaner signal [8], [15]. Sentinel-2 is a multispectral imaging mission of satellite (sentinel-2A) with capabilities including the Multispectral Instrument (MSI), which acquires free and open imagery in 13 spectral bands at resolutions of 10 m for visible and near-infrared (NIR) bands, 20 m for red-edge and SWIR (short-wave infrared) bands, and 60 m for atmospheric correction bands, with a common revisit frequency of every 5 days due to the high-resolution composite [16]. The COPERNICUS/S2_SR_HARMONIZED GEE collection contains a harmonization surface reflectance product, which provides bottom-of-atmosphere (BOA) corrected, radiometrically consistent, and analysis ready data [17]. The ten bands chosen to constitute the inputs for the RF classification were B2, B3, B4, B5, B6, B7, B8, B8A, B11, and B12, covering visible through red-edge to NIR and SWIR spectral domains, maximizing inter-class spectral discriminability. Fig 2 illustrates the true-color RGB and false-color near-infrared for visual interpretation and vegetation contrast enhancement.

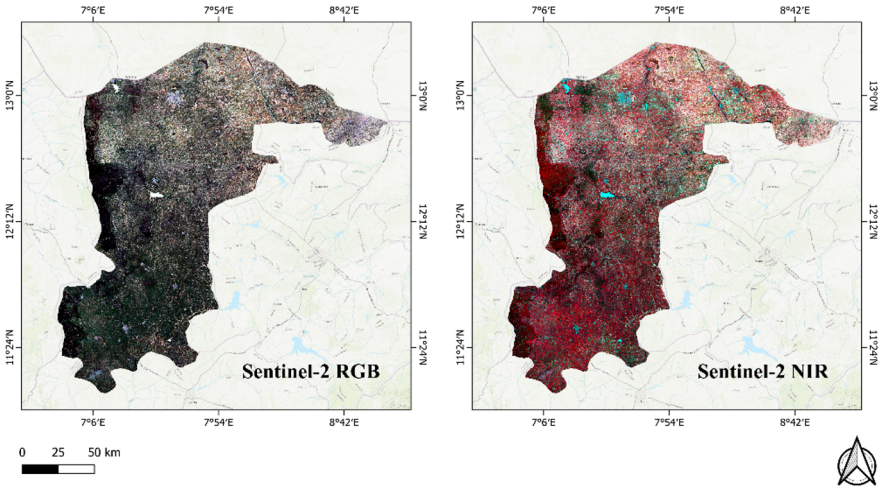

Fig. 2. Input composites of Sentinel-2 Satellite Imagery in true-color RGB, and False-color NIR for Katsina State

3 Methodology

3.1 Data Acquisition and Preprocessing

The dataset comprised Sentinel-2 Level-2A surface reflectance imagery (10 m spatial resolution) obtained from the COPERNICUS/S2_SR_HARMONIZED collection in GEE. The composite was generated from multiple images (<10% of cloud filtering). The image acquisition period was selected to coincide with the wet-to-dry season. This spectral contrast is caused by senescing vegetation, harvested croplands, and receding water bodies during this period [18] that help improve separability among the LULC

classes. To preserve the quality of our data, we eliminated scenes during dynamic filtering with more than 10% cloud cover. Then, a median composite and selected bands were applied to the remaining images of the selected temporal window to minimize residual atmospheric effect and obtain a radiometrically homogeneous composite image. The composite was then clipped to the administrative boundary of Katsina State to limit any further processing to the study area [19]. Composite imagery was used to generate training samples covering six LULC classes. Sample points were extracted at a 10 m spatial resolution using sampleRegions() function in GEE to generate spectral feature vectors for training a RF model of the entire study region [20].

3.2 Classification

The LULC classification framework considered six classes: water, vegetation (forest and grassland), barren, cropland, buildup, and arroyos. These categories were selected to represent the major land-cover types found in the semi-arid Sudan Savanna of the study area. Training samples for each class were generated through visual interpretation of Sentinel-2 imagery and supporting high-resolution satellite data within the GEE platform [21]. The randomColumn() function in GEE was then used to randomly split the samples into two subsets to prepare for classification. Common machine learning practices from remote sensing classification studies were followed, with 80% of the samples used for model training, and 20% served as an independent validation set [22]. The RF classifier was implemented using smartRandomForest() GEE method. The RF model consisted of 100 trees with default GEE parameters, employing bootstrap aggregation and random feature selection per split. The number of variables to split on was determined automatically as the square root of the total number of predictor variables. RF comprises an ensemble of machine learners that builds decision trees with each tree trained using bootstrap aggregation of the training data and random subsets of predictor variables at each node split [23]. Training and classification were executed with six LULC classes using stratified random sampling to reduce classification bias. The final class prediction is obtained through majority voting of all trees in the ensemble. This architecture allows RF to optimally classify high-dimensional spectral data, minimize overfitting, and be robust against noise or multicollinearity of the independent variables [24]. Consequently, RF has been used to successfully map disparate land-cover classes in semi-arid areas like Katsina State [25]. The trained model was used to classify the Sentinel-2 composite images at 10 m spatial resolutions, to produce the final LULC map for the study area [26]. The proposed methodology framework for Sentinel-2-based LULC Classification Using RF in GEE is shown in Fig 3.

3.3 Accuracy Assessment

An overall and per-class performance evaluation was conducted after the classification process with RF to assess the quality of the generated LULC map for Katsina State based on Sentinel-2 [17]. The 20% validation subset held out of the training process was passed through the trained RF model, and predicted labels were then compared to their known reference labels to construct a per-class confusion matrix directly within

the GEE environment [27]. The performance metrics were computed based on the confusion Matrix, and a complete set of evaluation statistics was retrieved using GEE's built-in accuracy assessment functions [28]. These included Overall Accuracy (OA), which measures how well the validation pixels were classified overall; Producer Accuracy (PA), and Omission Error (OE) [29], which together characterize how well each reference class was detected; User or Consumer Accuracy (CA) and Commission Error (CE), respectively capturing how faithfully a classified pixel belongs to its assigned category; and Kappa Coefficient (κ) [30], a statistic that corrects for chance agreement, meaning it provides a more truthful representation of classifier performance than OA alone. These metrics present a transparent and balanced representation of the RF classifier performance across the six LULC classes in the study area. All metrics were calculated directly from the confusion matrix that resulted from independent validation samples, thus providing an unbiased measure of performance.

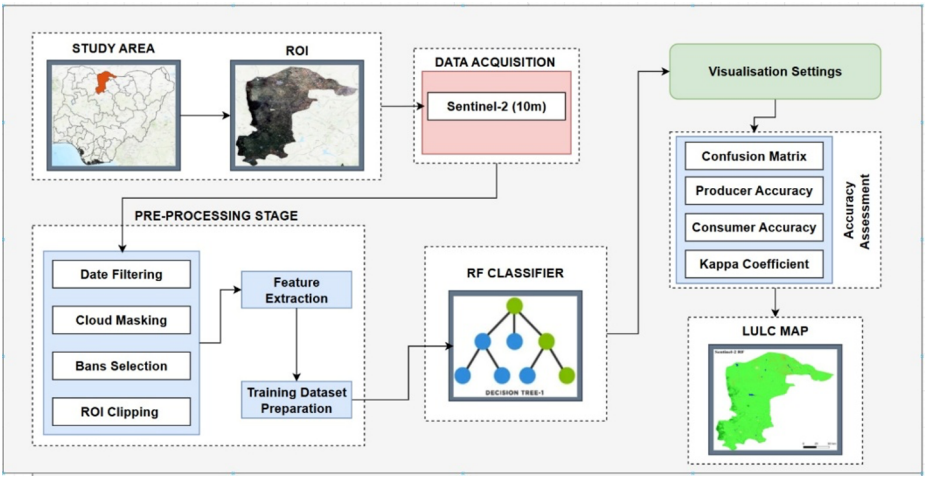

Fig.3. Proposed methodology framework of RF-Based LULC Classification over Sentinel-2 data in GEE of Katsina state, Nigeria.

4 Results

4.1 Visual Analysis

Fig 4 presents the LULC classification map for Katsina State, derived from Sentinel-2 surface reflectance using RF, with six land-cover classes: cropland, vegetation, water, barren, arroyos, and buildup. The most pronounced feature of this map is the cropland, which spans the northern, central, and eastern areas of the state, consistent with the fact that rain-fed subsistence agriculture is the largest land-cover activity in these regions. Vegetation, on the other hand, is predominantly found in the southwest and south, where marginally better moisture conditions facilitate denser woody and shrub cover characterizing the Sudan Savanna zone. This appears as small, dispersed patches with

limited spatial extent across the image, which is typical for imagery acquired in October during the wet-to-dry season transition, when surface water generally begins to recede. At the northern edge, bare land emerges as an isolated species in scattered patches; a symptom of ongoing vegetation regression associated with rising aridity and ongoing enthronization of the environment. In contrast, Arroyo features are generally limited in extent and appear as thin linear traces following seasonal drainage areas or dry water-beds. The buildup is therefore the least represented class on the map and appears as small, distinct clusters due to a low-density dispersed rural settlement pattern. The Sentinel-2 with a spatial resolution of 10 m contains enough detail for the classification map, allowing clear delineation of class boundaries and better detection of fragmented LULC features with minimal mixed-pixel effects.

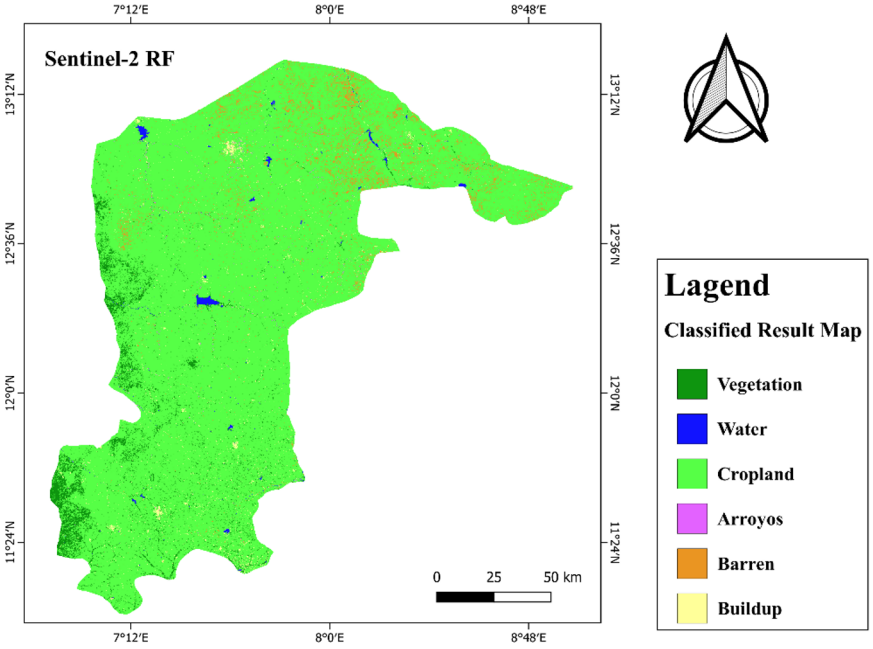

Fig.4. LULC Classification Map of Katsina State using RF Classifier and Sentinel-2.

4.2 Quantitative Analysis

The Geospatial classification in Katsina State was assessed using RF and the Sentinel-2 composite, which yielded an overall accuracy (OA) of 94.35% and a standard deviation of 0.02851, as shown in Table 1. The spread of its Confusion Matrix is illustrated in Fig. 5, denoting the great RF algorithm's power to discriminate between these six LULC types. On a class-by-class basis, water topped the list with a perfect PA of 100% and CA of 95.56%. This is hardly surprising as open water is one of the spectrally "unique" classes in both the NIR and SWIR. Vegetation and cropland were close in

score, with PA values of 99.36% and 98.45%, respectively, while OE values (OEs) on the order of 0.64% and 1.55% confirm that these ten bands from Sentinel-2 segments the dominant land cover types well during the October acquisition window.

Table 1. Assessment of Sentinel-2 Dataset for Katsina State, Nigeria Using RF Classifier Accuracy

Class	PA (%)	CA (%)	OE (%)	CE (%)
Water	100.00	95.56	0.00	4.44
Vegetation	99.36	93.33	0.64	6.67
Barren	46.34	68.89	53.66	31.11
Buildup	26.81	66.67	73.19	33.33
Arroyos	58.97	57.78	41.03	42.22
Cropland	98.45	95.56	1.55	4.44
			OA = 94.35%	**SD = 0.02851**

The shelf for buildup, barren, and arroyos, which together made up more than half of the confusion matrix misclassifications, looks markedly different. The buildup had the lowest score, PA was only 26.81%, CA 66.67%, and OE up to 73.19%. The problem here is that low-density impervious surfaces and bare post-harvest cropland look extremely similar in the dry season, making reliable separation nearly impossible. It had PA = 46.34% and CA = 68.89%, thus still not very high numbers, but better; however, barrens were even being confused with cropland, because barren land and exposed agricultural fields reflect similarly in the visible range and SWIR. If we use this non-overlap category as a leading threshold, arroyos emerge in the median results with 58.97% PA and 57.78% CA of these features not escaping the mixed-pixel effects endemic to narrowing seasonal drainage morphology mapped at 10 m resolution. Conclusively, these results suggest that the major limitation is consistent classification performance across the semi-arid domain of Katsina State and its spectral similarity under dry-season conditions.

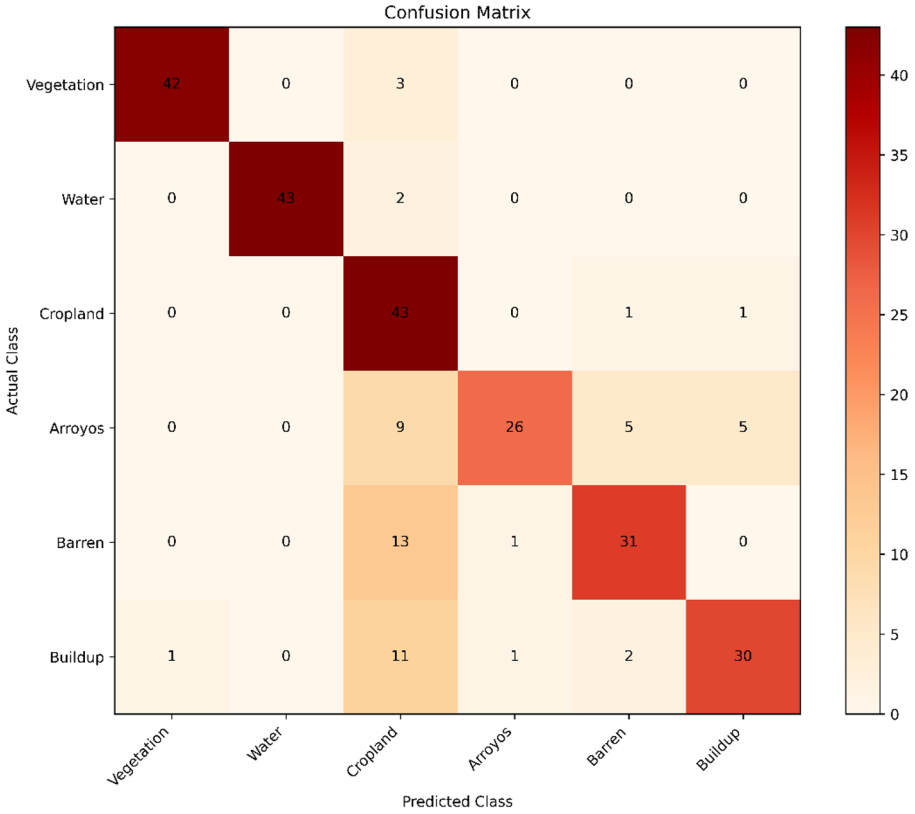

Fig.5. A Sentinel-2 RF Confusion Matrix for LULC Classification of Katsina State, Nigeria.

Under dry-season spectral conditions characterized by vegetation senescence and reduced surface moisture, classification performance was stable across land-covered types found in the most dominant environments.

5 Discussion

The accuracy assessment of 94.35% for the overall LULC classification using a RF classifier with Sentinel-2 composite imagery over Katsina State indicates good performance in mapping in a semi-arid setting. These performances indicate proper selection of the October 2025 acquisition window. That timing happens to fall smack in the late wet-to-dry seasonal transition, when fields cleared of harvest stand bare (vegetation is heavily senescent at the opposite end of the seasonal cycle), atmospheric moisture is dwindling; properties that collectively act to push spectral differences between land cover types apart and thereby simplify classification considerably. This is also evident in the three most positive classes: water, vegetation, and cropland. Water achieved the

highest producer's accuracy (PA) of 100% and commission error (CA) of 95.56%, which is due to the clear absorption characteristics of open water in near infrared reflectance (NIR) and short-wave infra-red reflectance (SWIR) bands; vegetation, as well as cropland, also acquired PA performance greater than 98%; this proves that RF can deal with spectrally separable and spatially prevailing classes evenly and reliant. The study OA of 94.35% is comparably consistent with similar semi-arid West African studies, in which RF classifications based on Landsat images from a single date have yielded OAs between 78 and 92% [31]. This performance improvement is fairly explained by the attributes of (i) GEE median compositing, (ii) Strategic acquisition time, and iii) more spectrometric data offered by 10 chosen Sentinel-2 bands. This study introduces some very practical considerations to the regional literature, beyond occulting numbers. It describes a GEE-based RF framework to Sentinel-2 imagery that generates consistent LULC maps with real value for land degradation assessment and evidence-based environmental governance in northwestern Nigeria.

That said, the findings for buildup, barren, and arroyos offer a more complicated picture that merits an honest dive. Once again, the lowest performance was from buildup, with only 26.81% PA and 73.19% OE. The problem itself is simple but not trivial to solve: low-density rural settlements are spectrally contaminated by the bare soil and sparse vegetation surrounding them, rendering them spectroscopically similar to exposed post-harvest cropland fields at a 10 m pixel scale. The RF classifier just had too few clean spectral signals to learn from. Barren faced a comparable issue, recording a PA of 46.34% (most of its misclassification fell into the cropland category), not surprising given that barren and harvested fields exhibit very similar reflectance profiles across the visible and SWIR regions under dry season conditions. Arroyos themselves resulted in a PA of 58.97%; their narrow linear geometry means that at 10 m resolution, many arroyos' pixels contain mixed signals from adjacent types, corresponding to classification errors along class boundaries. Potential improvements in future work to address these weaknesses will probably involve including more data sources: topographically based digital elevation models, spectral indices of vegetation and moisture (eg, NDVI, NDWI, NDBI), and denser class-stratified training samples would all provide a better chance for the RF classifier when attempting to distinguish spectrally ambiguous classes across the semi-arid landscape of Katsina State.

6 Conclusion

The study presented here demonstrates that RF classification produces reliable LULC of the semi-arid landscape of Katsina State, northwestern Nigeria, using Sentinel-2 satellite imagery in GEE. It provides an overall accuracy of 94.35% and a standard deviation of 0.02851, with high PA values for water, vegetation, and cropland, 100%, 99.36%, and 98.45%, respectively, due to the strategic acquisition window in October as well as the wide spectral coverage of Sentinel-2 data. Aggregate accuracy metrics alone cannot capture classifier performance in spectrally complex landscapes, with buildup, barren, and arroyos performing poorly for dry-season spectral similarity with cropland. The GEE-based RF framework validated in this study has direct practical

value for monitoring land degradation, managing agricultural land use, and implementing environmental governance within northwestern Nigeria.

References

1. I. Shandu, S. Xulu, and M. Gebreslasie, "Enhancing land cover classification in the heterogeneous landscape by integrating auxiliary data with Sentinel-2 imagery using the random forest algorithm," Front. Remote Sens., vol. 6, pp. 1–27, Jan. 2026, doi: 10.3389/frsen.2025.1697897.
2. P. Harani, S. Gautam, S. K. Joshi, and C.-H. Ho, "Spatio-temporal analysis of land use transformations and their environmental implications in the Thamirabarani River Basin, India," Front. Remote Sens., vol. 6, Jan. 2026, doi: 10.3389/frsen.2025.1732414.
3. C. O. Oluseyi, S. S. Usman, and N. Y. Ngurnoma, "Geospatial Analysis of Land Use and Land Cover Changes Over Daura, Katsina State," Feb. 19, 2026, Research Square. doi: 10.21203/rs.3.rs-8893548/v1.
4. B. G. Saulawa, "Spatio-Temporal Vegetation Cover Change as an Analytic Technique for Appraising Desertification in Katsina State, Nigeria," Int. J. Sci. Res. Publ. IJSRP, vol. 8, no. 11, Nov. 2018, doi: 10.29322/IJSRP.8.11.2018.p8313.
5. I. Abbas, "Mapping Land Use-land Cover and Change Detection in Kafur Local Government, Katsina, Nigeria (1995-2008) Using Remote Sensing and Gis," Res. J. Environ. Earth Sci., Jan. 2010.
6. D. Phiri, M. Simwanda, S. Salekin, V. R. Nyirenda, Y. Murayama, and M. Ranagalage, "Sentinel-2 Data for Land Cover/Use Mapping: A Review," Remote Sens., vol. 12, no. 14, Jul. 2020, doi: 10.3390/rs12142291.
7. A. E. Fentaw and A. Abegaz, "Analyzing Land Use/Land Cover Changes Using Google Earth Engine and Random Forest Algorithm and Their Implications to the Management of Land Degradation in the Upper Tekeze Basin, Ethiopia," Sci. World J., vol. 2024, no. 1, p. 3937558, 2024, doi: 10.1155/2024/3937558.
8. E. Belcore and M. Piras, Sentinel 2 High-Resolution Land Cover Mapping in Sub-Saharan Africa with Google Earth Engine. 2023, p. 36. doi: 10.5220/0011746500003473.
9. B. Mutale, N. C. Withanage, P. K. Mishra, J. Shen, K. Abdelrahman, and M. S. Fnais, "A performance evaluation of random forest, artificial neural network, and support vector machine learning algorithms to predict spatio-temporal land use-land cover dynamics: a case from lusaka and colombo," Front. Environ. Sci., vol. 12, Sep. 2024, doi: 10.3389/fenvs.2024.1431645.
10. O. M. Alegbeleye, Y. O. Rotimi, P. Shomide, A. Oyediran, O. Ogundipe, and A. Akintunde-Alo, "Land use land cover (LULC) analysis in Nigeria: a systematic review of data, methods, and platforms with future prospects," Bull. Natl. Res. Cent., vol. 48, no. 1, p. 127, Dec. 2024, doi: 10.1186/s42269-024-01286-z.
11. A. Dahiru, A. H. Abdullahi, N. Bello, and M. L. Abubakar, "Assessment of the influence of climate change on desertification in Katsina state, Nigeria," Discov. Geosci., vol. 4, no. 1, p. 29, Jan. 2026, doi: 10.1007/s44288-026-00403-x.
12. K. Abubakar, I. B. Abaje, and R. Tukur, "RAINFALL AND TEMPERATURE DYNAMICS IN THE CONTEXT OF CLIMATE CHANGE IN THE SUDAN SAVANNA ECOLOGICAL ZONE OF KATSINA STATE, NIGERIA," FUDMA J. Earth Environ. Sci., vol. 1, no. 02, pp. 82–98, Dec. 2024, doi: 10.33003/jees.2024.0102/08.

13. D. O. Edokpa, P. N. Ede, B. E. Diagi, and S. I. Ajiere, "Rainfall and Temperature Variations in a Dry Tropical Environment of Nigeria," J. Atmospheric Sci. Res., vol. 6, no. 2, pp. 50–57, Apr. 2023, doi: 10.30564/jasr.v6i2.5527.
14. L. N. Sambe, C. O. Adeofun, J. A. Oyedepo, B. A. Osunmadewa, and J. A. Soaga, "Evaluation of desertification dynamics in the frontline states of Northern Nigeria: environmental and socioeconomic impacts," Environ. Res. Commun., vol. 8, no. 2, p. 025002, Feb. 2026, doi: 10.1088/2515-7620/ae322b.
15. B. T. Haile, A. Ramoelo, A. J. Dougill, and M. Qabaqaba, "Land Use/Land Cover (LULC) Change and Irrigated Area Monitoring in Eritrea: Insights into Horticultural Production and Sustainability," Remote Sens. Earth Syst. Sci., vol. 8, no. 4, pp. 1244–1264, Dec. 2025, doi: 10.1007/s41976-025-00247-y.
16. B. T. Mudereri et al., "Integrating the Strength of Multi-Date Sentinel-1 and -2 Datasets for Detecting Mango (Mangifera indica L.) Orchards in a Semi-Arid Environment in Zimbabwe," Sustainability, vol. 14, no. 10, May 2022, doi: 10.3390/su14105741.
17. A. Kumar, P. Sharma, N. Vyas, A. Sharma, R. Maheshwari, and P. K. Dutta, "Land Use Land Cover Mapping Using Random Forest and Multispectral Satellite Imagery in Google Earth Engine," in 2025 Third International Conference on Networks, Multimedia and Information Technology (NMITCON), Aug. 2025, pp. 1–5. doi: 10.1109/NMITCON65824.2025.11188013.
18. V. Nasiri, A. Deljouei, F. Moradi, S. M. M. Sadeghi, and S. A. Borz, "Land Use and Land Cover Mapping Using Sentinel-2, Landsat-8 Satellite Images, and Google Earth Engine: A Comparison of Two Composition Methods," Remote Sens., vol. 14, no. 9, Apr. 2022, doi: 10.3390/rs14091977.
19. O. Hagolle et al., "SENTINEL-2 Surface Reflectance Products Generated by CNES and Dlr: Methods, Validation and Applications," ISPRS Ann. Photogramm. Remote Sens. Spat. Inf. Sci., vol. 51, pp. 9–15, 2021, doi: 10.5194/isprs-annals-V-1-2021-9-2021.
20. M. Vizzari, "PlanetScope, Sentinel-2, and Sentinel-1 Data Integration for Object-Based Land Cover Classification in Google Earth Engine," Remote Sens., vol. 14, no. 11, May 2022, doi: 10.3390/rs14112628.
21. C. B. Pande et al., "Characterizing land use/land cover change dynamics by an enhanced random forest machine learning model: a Google Earth Engine implementation," Environ. Sci. Eur., vol. 36, no. 1, p. 84, Apr. 2024, doi: 10.1186/s12302-024-00901-0.
22. J. Svoboda, P. Štych, J. Laštovička, D. Paluba, and N. Kobliuk, "Random Forest Classification of Land Use, Land-Use Change and Forestry (LULUCF) Using Sentinel-2 Data—A Case Study of Czechia," Remote Sens., vol. 14, no. 5, Feb. 2022, doi: 10.3390/rs14051189.
23. L. Breiman, "Random Forests," Mach. Learn., vol. 45, no. 1, pp. 5–32, Oct. 2001, doi: 10.1023/A:1010933404324.
24. [24] A. Htitiou et al., "The Performance of Random Forest Classification Based on Phenological Metrics Derived from Sentinel-2 and Landsat 8 to Map Crop Cover in an Irrigated Semi-arid Region," Remote Sens. Earth Syst. Sci., vol. 2, no. 4, pp. 208–224, Dec. 2019, doi: 10.1007/s41976-019-00023-9.
25. [25] K. Abida et al., "Sentinel-2 Data for Land Use Mapping: Comparing Different Supervised Classifications in Semi-Arid Areas," Agriculture, vol. 12, no. 9, Sep. 2022, doi: 10.3390/agriculture12091429.
26. [26] A. F. Jocea, L. Porumb, L. Necula, and D. Raducanu, "Sentinel-2 Land Cover Classification: State-of-the-Art Methods and the Reality of Operational Deployment—A Systematic Review," Sustainability, vol. 17, no. 22, Nov. 2025, doi: 10.3390/su172210324.

27. A. P. Nicolau, K. Dyson, D. Saah, and N. Clinton, "Accuracy Assessment: Quantifying Classification Quality," in Cloud-Based Remote Sensing with Google Earth Engine: Fundamentals and Applications, J. A. Cardille, M. A. Crowley, D. Saah, and N. E. Clinton, Eds., Cham: Springer International Publishing, 2024, pp. 135–145. doi: 10.1007/978-3-031-26588-4_7.
28. "Geospatial Data Science," Geospatial Data Science. Accessed: Mar. 08, 2026. [Online]. Available: https://blog.gishub.org
29. G. Amin, I. Imtiaz, E. Haroon, N. us Saqib, M. I. Shahzad, and M. Nazeer, "Assessment of Machine Learning Algorithms for Land Cover Classification in a Complex Mountainous Landscape," J. Geovisualization Spat. Anal., vol. 8, no. 2, p. 34, Aug. 2024, doi: 10.1007/s41651-024-00195-z.
30. B. Feizizadeh, S. Darabi, T. Blaschke, and T. Lakes, "QADI as a New Method and Alternative to Kappa for Accuracy Assessment of Remote Sensing-Based Image Classification," Sensors, vol. 22, no. 12, Jun. 2022, doi: 10.3390/s22124506.
31. E. A. Lawer, "An evaluation of single and multi-date Landsat image classifications using random forest algorithm in a semi-arid savanna of Ghana, West Africa," Sci. Afr., vol. 26, p. e02434, Dec. 2024, doi: 10.1016/j.sciaf.2024.e02434.